Orbital rotational vibrations in the $A = 130$ mass region

Amand Faessler and Roland Nojarov*
Institut für Theoretische Physik, Universität Tübingen, Auf der Morgenstelle 14, D-7400 Tübingen, Federal Republic of Germany
(Received 5 June 1989)

The rotational vibrations ($K^\pi = 1^+$ states) in 16 even-even Xe, Ba, and Ce nuclei are studied in the quasiparticle random-phase approximation with a mean field given by a deformed Woods-Saxon potential and residual forces: a self-consistent quadrupole-quadrupole interaction, a spin-spin interaction, and a force that restores the rotational invariance of the Hamiltonian. A shell effect is found which is typical for this mass region: a strong orbital character of almost all low-energy (2.5–5 MeV) excitations, while the higher-energy ones are predominantly spin flip. The comparison of random-phase approximation $M1$ transition densities and (e,e') form factors with the microscopic realization of the two-rotor model 1^+ state allow us to conclude that the strongly orbital low-energy random-phase approximation states perform the scissor-type motion described by the two-rotor model, but only few particles are involved in this motion.

I. INTRODUCTION

In addition to the usual beta and gamma vibrations with $K^\pi = 0^+$ and 2^+, respectively, oscillations with $K^\pi = 1^+$ are also possible in deformed nuclei. In the simple geometrical picture of the collective model[1] they are generated by a deformation change, produced by the Q_{21} operator and have, therefore, the meaning of rotational vibrations around an axis, which is perpendicular to the symmetry axis of the nucleus. Due to the rotational invariance of the Hamiltonian and to the fact that one works in the intrinsic system, such a motion is forbidden in the isoscalar collective model, which assumes that the neutrons and the protons move always together and can, therefore, be described by a common isospin-independent collective coordinate. Thus, no quadrupole-quadrupole interaction was present in some of the first microscopic random-phase approximation (RPA) calculations[2,3] of the 1^+ states in deformed nuclei and the states were obtained with a spin-spin interaction alone. Such an interaction was used previously[4] to generate spin-vibrational 1^+ states in the spherical nucleus ^{208}Pb. However, rotational vibrations are allowed in the collective model if one generalizes it to include isospin-dependent coordinates in order to describe out-of-phase neutron-proton vibrations.[5] Due to this reason, a quadrupole-quadrupole residual interaction, based on the Q_{21} operator, was also used in microscopic calculations[6–11] to generate 1^+ states. The spin-spin (SS) interaction is present, together with the quadrupole-quadrupole (QQ) interaction and an RPA approach, in a number of works.[6–9] It is also a part of the density-dependent Landau-Migdal interaction, which was used for the microscopic description of 1^+ states as well.[12,13] The numerical results, reported in the latter reference, were obtained, however, without a spin-spin interaction.

Additional simplifying assumptions, which reduce the order of the RPA secular equation, have been made about the coupling constants of the SS interaction in most of the above works. The assumption of equal neutron-neutron, proton-proton, and neutron-proton coupling constants [$c_{nn} = c_{pp} = c_{np}$] (Refs. 6 and 9) closes the isovector channel [$c(1) = c_{nn} - c_{np} = 0$] of the SS interaction and one is left with the isoscalar channel only [$c(0) = c_{nn} + c_{np} = 2c_{nn}$]. The assumption of vanishing neutron-proton interaction [$c_{np} = 0$] (Ref. 3) leads formally to equal isoscalar and isovector strength constants [$c(1) = c(0)$] but in fact the absence of the neutron-proton coupling term means that this interaction is not able to generate coherent isovector vibrations, which require a neutron-proton restoring force. The more general case $c_{nn} = c_{pp} \neq c_{np}$ is considered only in Refs. 2, 7, and 8. The latter one, as well as Ref. 6, being purely theoretical studies, do not report any numerical results.

In the case of beta and gamma vibrations there is a freedom in the choice of the interaction strength constants, which are usually fitted to the experimental energy of the first strongly collective vibrational state. In contrast, the 1^+ excitations, although less collective, have a more fundamental character, because they are closely related to the condition of rotational invariance of the Hamiltonian. Thus, the obtained RPA phonon wave functions have to be orthogonal to the zero-energy spurious state,[14] which corresponds to isoscalar rotation of the nucleus as a whole. As a result, no freedom is left for the quadrupole-quadrupole interaction strengths and the resulting RPA 1^+ states happen to be almost purely isovector.[11] The very important question of restoration of the rotational invariance, which is broken by the deformed mean field, was ignored in a number of works.[2,3,13] At most, a zero-energy solution of the secular equation was asked in some of them, which is not sufficient to ensure orthogonality of the RPA excitations with respect to the spurious state, created by the angular momentum operator. As a result, most of the 1^+ states have large spurious isoscalar admixtures.

Results, obtained after restoration of the rotational invariance, were reported in Refs. 7, 9, 11, and 12. The

method of Ref. 7 has not a general validity. It works only with a mean field in the form of a Nilsson potential. In this case a suitable choice of the quadrupole-quadrupole constant allows one to express exactly the angular momentum matrix elements through the quadrupole ones. The method does not work for a Woods-Saxon potential. Moreover, all the three quadrupole force constants have to be set equal ($k_{nn}=k_{pp}=k_{np}$), which is a particular case and closes the isovector channel. In contrast, a self-consistent determination of the quadrupole strengths[10,11] leads to three different values.

Two methods of general validity were proposed: a restoration of the rotational symmetry of the quasiparticle Hamiltonian[9,12] by commuting it with the angular momentum or the conjugate angle operator, respectively, and a restoration of the rotational invariance of the RPA Hamiltonian[11] by orthogonalizing the phonon wave functions with respect to the spurious state. Our method[11] was used until now with a QQ interaction alone. We apply it here to a Hamiltonian, which contains a spin-spin force as well and we study the rotational vibrations in the Xe-Ba-Ce region. We were motivated for this study also by our preliminary results for three Ba nuclei,[15] which showed the presence of low-energy rotational vibrations with a very strong orbital character (the orbital angular momentum matrix element is one order of magnitude larger than the spin one). The experimental orbit-to-spin ratio in several rare-earth nuclei and ^{46}Ti is 1–4 (Ref. 16) and only in ^{156}Gd a large ratio (20–45) was found.[17] Thus, in the present work we are particularly interested in a possible enhancement of the orbit-to-spin ratio through the spin-spin interaction.

In the following section we discuss our formalism and in Sec. III we choose the constants of the spin-spin interaction after a short review of previous works. The numerical procedure, the results for $M1$ strength distributions, and the effects of the spin-spin interaction are discussed in Sec. IV. Comparison with the two-rotor model, based on $M1$ transition densities and (e,e') form factors, is given in Sec. V.

II. RESTORATION OF ROTATIONAL INVARIANCE

We considered already the case of quadrupole-quadrupole residual interaction alone in Ref. 11, where our method for the restoration of the rotational invariance of the Hamiltonian on the RPA level was formulated. Let us introduce now additionally a spin-spin interaction of the form

$$\begin{aligned} H_{\rm SS}&=-\tfrac{1}{2}\sum_m m\,[c(+,n)S^2(m,n)+c(+,p)S^2(m,p)\\ &\qquad +2c(-)S(m,n)S(m,p)],\\ S(m,t)&=\tfrac{1}{2}[S_+(t)-mS_-(t)],\quad m=\pm 1\ ,\\ S(m,t)&=\begin{cases} iS_y(t), & \text{for } m=+1\ ,\\ S_x(t), & \text{for } m=-1\ ,\end{cases}\\ S(m)&=\sum_t S(m,t),\quad t=n,p\ , \end{aligned} \tag{1}$$

where m is a signature index, t is an isospin index, and $c(+,n),c(+,p),c(-)$ are the neutron-neutron, proton-proton, and neutron-proton interaction strengths, respectively. If the first two of these constants are chosen equal, which has been always the common choice,[2,3,7,9,12] the interaction (1) acquires the more symmetric form:

$$\begin{aligned} &H_{\rm SS}=\tfrac{1}{2}\sum_{m,\tau} c(\tau)S^\dagger(m,\tau)S(m,\tau)\ ,\\ &S(m,\tau)=S(m,n)+(-1)^\tau S(m,p),\quad \tau=0,1\ ,\\ &c(0)=\tfrac{1}{2}[c(+)+c(-)],\quad c(1)=\tfrac{1}{2}[c(+)-c(-)],\quad c(+)=c(+,n)=c(+,p)\ , \end{aligned} \tag{2}$$

with isoscalar ($\tau=0$) and isovector ($\tau=1$) channels. The quasiboson representation of the spin operator has the same quasiparticle structure as that of the angular momentum operator:[11]

$$\begin{aligned} &S(m,t)=\sum_{ik}\{s(ki,mt)[A^\dagger(k,mt)-mA(ik,mt)]+s(\tilde{k}i,mt)[\overline{A}^\dagger(ik,mt)-m\overline{A}(ik,mt)]\}\ ,\\ &A^\dagger(ik,mt)=(\alpha_{\tilde{i}}^\dagger\alpha_k^\dagger-m\alpha_i^+\alpha_{\tilde{k}}^+)_t/\sqrt{2},\quad \overline{A}^\dagger(ik,mt)=(\alpha_{\tilde{k}}^\dagger\alpha_{\tilde{i}}^\dagger+m\alpha_k^\dagger\alpha_i^\dagger)_t/\sqrt{2}\ ,\\ &s(ki,mt)=-v(k,i)\langle k|S(m,t)|i\rangle/\sqrt{2},\quad s(\tilde{k}i,mt)=v(k,i)\langle\tilde{k}|S(m,t)|i\rangle/\sqrt{2}\ ,\\ &v(k,i)=u_kv_i-u_iv_k,\quad \alpha_{\tilde{i}}^\dagger=T\alpha_i^\dagger T^{-1}\ , \end{aligned} \tag{3}$$

where T is the time-reversal operator and $\alpha^\dagger$ are quasiparticle creation operators.

The model Hamiltonian has the form

$$\begin{aligned} &H=H_0+H_{\rm SCQ}+H_{\rm SS}+H_{\rm RV}\ ,\\ &H_{\rm SCQ}=-\tfrac{1}{2}\sum_m m\,[k(+,n)Q^2(m,n)+k(+,p)Q^2(m,p)+2k(-)Q(m,n)Q(m,p)]\ ,\\ &H_{\rm RV}=\tfrac{1}{2}\sum_{\nu,m} k(\nu,m)I^\dagger(m)[\Gamma^\dagger(\nu m)-m\Gamma(\nu m)]\ , \end{aligned} \tag{4}$$

where H_0 is the deformed mean field plus pairing. H_{SCQ} is in the sense of Eq. (41) of Ref. 11 a self-consistent quadrupole-quadrupole residual interaction and H_{RV} is a rotation-vibrational coupling. The strength constants of H_{SCQ} are determined fully microscopically[11] (no free parameters) from the condition of approximate restoration of the rotational invariance and all the three of them $[k(+,n),k(+,p),k(-)]$ are in general different. The condition, which is used for their determination [Eq. (41) in Ref. 11], is not affected by the additional inclusion of the spin-spin interaction now, since this interaction commutes with the total angular momentum operator $I(m)$. Moreover, this condition is fulfilled now in the RPA approximation due to the rotational invariance of the RPA Hamiltonian, following from Eq. (5). The coupling constants $k(\nu,m)$ of the symmetry restoring interaction H_{RV} have the meaning of Lagrange multipliers and are determined from the additional condition

$$[I(m),\Gamma^{\dagger}(\nu m')]=0 \ . \tag{5}$$

It ensures the orthogonality of the RPA wave functions, created by the phonon operators $\Gamma^{\dagger}(\nu m)$ (8) with respect to the spurious state, created by the angular momentum operator $I(m)$. As a result, the RPA Hamiltonian becomes rotationally invariant and the $M1$ transitions are almost purely isovector.[11,18] The explicit form of H_0, $Q(m,t)$, and $I(m)$ can be found in Ref. 11.

The quasiparticle RPA equations of motion

$$[H,\Gamma^{\dagger}(\nu m)]=W_{\nu}\Gamma^{\dagger}(\nu m) \ , \tag{6}$$

$$[\Gamma(\nu m),\Gamma^{\dagger}(\nu' m')]=\delta(\nu,\nu')\delta(m,m') \ , \tag{7}$$

are solved together with the constraint (5) and the usual ansatz[11] for the phonon creation operator

$$\begin{aligned}\Gamma^{\dagger}(\nu m)=\tfrac{1}{2}\sum_{ik,t}[&\psi_{\nu}(ki,mt)A^{\dagger}(ik,mt)-\phi_{\nu}(ki,mt)A(ik,mt)\\&+\lambda_{\nu}(ki,mt)\overline{A}^{\dagger}(ik,mt)\\&-\mu_{\nu}(ki,mt)\overline{A}(ik,mt)] \ .\end{aligned} \tag{8}$$

The RPA Eqs. (5) and (6) determine the phonon amplitudes (8):

$$\begin{aligned}&\psi_{\nu}(ki,mt)=[N(\nu,t)q(ki,mt)-L(\nu,m,t)s(ki,mt)-k(\nu,m)j(ki,mt)]/[E(ik)-W_{\nu}] \ ,\\&\phi_{\nu}(ki,mt)=m[N(\nu,t)q(ki,mt)+L(\nu,m,t)s(ki,mt)+k(\nu,m)j(ki,mt)]/[E(ik)+W_{\nu}] \ ,\\&E(ik)=E(i)+E(k) \ ,\end{aligned} \tag{9}$$

and λ,μ, which follow from (9) after substituting in the right-hand side (rhs) $(ki)\rightarrow(\tilde{ki})$. $E(i)$ are quasiparticle energies. $N(\nu,t)$ and $L(\nu,m,t),t=n,p$ are unknown quadrupole and spin norms, respectively, which have to be determined together with the Lagrange multipliers $k(\nu,m)$, i.e., a total of five unknowns. Equations (5) and (6) form a linear homogeneous system with respect to the above five unknowns and the RPA secular equation is obtained by asking that the corresponding 5×5 determinant, which is given in the Appendix (A1), vanishes. The secular equation, which determines the 1^+ excitation energies W_{ν}, has the following analytical form:

$$\begin{aligned}&gh+W_{\nu}^2A+W_{\nu}^4D=0 \ ,\\&g=[1+B_{ss}(+,n)][1+B_{ss}(+,p)]-B_{ss}(-,n)B_{ss}(-,p) \ ,\\&h=[1-B_{qq}(+,n)][1-B_{qq}(+,p)]-B_{qq}(-,n)B_{qq}(-,p) \ ,\\&A=A(n)+A(p), \quad A(t)=p(q,t)p(s,t)+v(q,-t)v(s,t) \ ,\\&D=[B_{qj}(+,n)B_{qj}(+,p)-B_{qj}(-,n)B_{qj}(-,p)][B_{sj}(+,n)B_{sj}(+,p)-B_{sj}(-,n)B_{sj}(-,p)] \ ,\\&p(q,t)=B_{qj}(+,t)[1-B_{qq}(+,-t)]+B_{qj}(-,t)B_{qq}(-,-t) \ ,\\&p(s,t)=B_{sj}(+,t)[1+B_{ss}(+,-t)]-B_{sj}(-,t)B_{ss}(-,-t) \ ,\\&v(q,t)=B_{qj}(-,t)+B_{qj}(+,t)B_{qq}(-,t)-B_{qj}(-,t)B_{qq}(+,t) \ ,\\&v(s,t)=B_{sj}(-,t)-B_{sj}(+,t)B_{ss}(-,t)+B_{sj}(-,t)B_{ss}(+,t) \ ,\end{aligned} \tag{10}$$

where the B sums are given by (A3). The terms with A and D do not vanish only when both the QQ and SS interactions are present in the Hamiltonian (4), otherwise the secular equation (10) has the form $g=0$ for a spin-spin interaction only, or $h=0$ for a quadrupole-quadrupole interaction alone. The latter case coincides with the secular equation of our previous work,[11] where no spin-spin interaction was present.

Let us note some more particular cases, possessing higher symmetry. When the QQ interaction constants are chosen self-consistently, which has always been done in our numerical calculation, reported in Secs. IV and V, a relation takes place:[11]

$$k(+,n)k(+,p)=k^2(-) \ . \tag{11}$$

The relations (A5) and (A6), which follow from (11), satisfy the secular equation (10) and it now takes the form

$$gh + W_\nu^2 A = 0 ,$$
$$h = 1 - B_{qq}(+,n) - B_{qq}(+,p) . \quad (12)$$

Our numerical results are obtained with this secular equation. The same form (12) of the secular equation is obtained if, instead of (11), the relation

$$c(+,n)c(+p) = c^2(-) \quad (13)$$

is satisfied, but now the function g takes a simpler form:

$$g = 1 + B_{ss}(+,n) + B_{ss}(+,p) . \quad (14)$$

Further simplifications can be obtained if all the three coupling constants are chosen equal. Each one of the assumptions $k = k(+,n) = k(+,p) = k(-)$ and $c = c(+,n) = c(+,p) = c(-)$ reduces the order of the determinant (A1) by one unity and if both of them are made, one is left with a much simpler 3×3 system. We do not consider such cases here because the above assumptions close the isovector channel for both the QQ and SS interactions.

Once the excitation energy W_ν is found for the $\nu^{-\text{th}}$ excited phonon state from the secular equation (10), one can determine the five unknowns $N(\nu,t), L(\nu,m,t), k(\nu,m), t = n,p$ from the normalization condition (7), as explained in the Appendix [(A7) and (A8)]. Afterwards, the RPA phonon amplitudes are determined from (9) and one is able to calculate all the possible physical observables, e.g., transition probabilities, transition densities, etc., with the obtained RPA wave function, using the formalism, developed in Ref. 11.

The form of the expressions for the RPA sum rules, given there, obviously does not change. The SS interaction does not contribute to the $M1$ quasiparticle sum rule. The quasiparticle energy-weighted sum rule for the $E2$ operator has the form

$$S_{\text{QPEW}}(E2) = [Q_{2m}^\dagger, [H, Q_{2m}]]_{qp} = 2\sum_t e^2(t) P_{qq}(t) + 2\sum_t e(t) f(t) P_{qs}(t) + \left[\sum_t e(t) P_{qj}(t)\right] \sum_\nu k(\nu,m) \left[\sum_t e(t) P(\nu,m,t)\right] ,$$
$$P_{qq}(t) = 4\sum_{ik} E(ik)[q^2(ki,mt) + q^2(\tilde{k}i,mt)] ,$$
$$P_{qu}(t) = 4m \sum_{ik} [q(ki,mt)u(ki,mt) + q(\tilde{k}i,mt)u(\tilde{k}i,mt)], \quad (u) = (s),(j) ,$$
$$f(t) = c(+,t) P_{qs}(t) e(t) + c(-) P_{qs}(-t) e(-t) , \quad (15)$$
$$P(\nu,m,t) = 4\sum_{ik} [F_\nu(ki,mt) q(ki,mt) + F_\nu(\tilde{k}i,mt) q(\tilde{k}i,mt)] ,$$
$$e(n) = e_{\text{eff}}, \quad e(p) = 1 + e_{\text{eff}} ,$$

where $e(t)$ are effective charges and $F_\nu(ki,mt)$ are linear combinations of the phonon amplitudes (9), defined by (A4) of Ref. 11. The first term of $S_{\text{QPEW}}(E2)$ comes from contribution of the mean-field H_0, the second one from H_{SS}, and the third one from H_{RV}.

III. THE STRENGTH OF THE SPIN-SPIN INTERACTION

The condition of rotational invariance, which was used[11] to determine the strength constants of the quadrupole-quadrupole force, cannot determine the constants of the spin-spin force, because this latter interaction is rotationally invariant. A brief review of the values of these constants, published previously, is given in Table I. Although it is far from complete, one can see that quite different values are required when the spin-spin interaction is used to describe different phenomena. Since nobody reported three different SS constants, which are allowed by our formalism, we assume from now on that

$$c(+,n) = c(+,p) = c(+) . \quad (16)$$

After this choice, the following relations can be established between our constants [(1) and (16)] and those from Table I, used in Ref. 19:

$$c(\pm) = 4V_0(\pm) , \quad (17)$$

in Refs. 2, 3, 7, 8, and 20–22:

$$c(+) = 8\kappa, \quad c(-) = 8q\kappa , \quad (18)$$

and in Refs. 12, 23, and 24–31:

$$c(\pm) = 8NC(g_0 \pm g'), \quad N = 1/V = 3/(4\pi r_0^3 A) . \quad (19)$$

Table I was prepared using the relations (17)–(19) and renormalizing all the quoted spin constants of the Landau-Migdal interaction to "pionic units"[31] $C = 392$ MeV fm^3.

In order to compare the density-dependent Landau-Migdal interaction with our density-independent spin-spin interaction, we assume a constant density distribution inside a sphere with radius $R = r_0 A^{1/3}$. After integrating the spin-spin part of the Landau-Migdal interaction over this volume, one obtains the following density-independent interaction:

$$H_{\text{LM}} = NC(g_0 \boldsymbol{\sigma}\cdot\boldsymbol{\sigma} + g' \boldsymbol{\sigma}\cdot\boldsymbol{\sigma}\boldsymbol{\tau}\cdot\boldsymbol{\tau}) , \quad (20)$$

with N given by Eq. (19). Comparison with (1) leads to (19), which is, of course, a rough estimate.

The upper part of Table I (cases b, c, e, and f) refers to separable spin-spin interactions of the type we use here, while the lower part refers to the Landau-Migdal force. Since in most approaches $c(+) = K_s/A$, we list only the mass-independent constant K_s in Table I. As one can see, this constant varies in the range 100–600 MeV. The ratio

$q=c(-)/c(+)$ covers the range $-1.5\leq q\leq 0$. This means that the neutron-neutron and proton-proton spin-spin interactions are repulsive, while the neutron-proton one is attractive (let us remember that all the three corresponding quadrupole forces are attractive).

The early works[19,20–22] were describing magnetic dipole moments and decoupling parameters of odd-mass rare-earth nuclei. Later microscopic calculations of 1^+ states[2,7] take the values from Ref. 20. Analogous calculations[3,9] adopt the isovector dependence $\kappa=1.5(N-Z)/2A$. The spin constants of the Landau-Migdal interaction, used in similar calculations[12] (case f), were taken also from previous works, describing magnetic moments of spherical and deformed nuclei. Cases g (Ref. 24) and h (Ref. 25) from Table I reproduce electromagnetic transitions and g factors of nuclei from the Pb region, while the next four works[26–29] deal with nuclear matter calculations, the first two considering mechanisms, preventing pion condensation. These four works do not fit the Landau-Migdal strengths to experimental data but obtain them from G-matrix calculations including interactions, induced from isobars. The first three works use the Brueckner-Hartree-Fock (BHF) approach. The latter two include relativistic corrections. In spite of the fact that the isoscalar strength g_0 varies from -0.12 to $+0.15$, having in view the large uncertainty of the strengths, one can say that the results of these four fully microscopic calculations are in a good agreement with each other. The isovector strength g' varies in the region $0.4\leq g'\leq 0.56$ and the isoscalar strength g_0 has a much smaller absolute value. However, in cases j (Ref. 28) and l (Ref. 27) the microscopically obtained ratio q is in a better agreement with the phenomenological values of q from g factor and decoupling parameter calculations b, c, e, and f in Table I.

In case m (Ref. 30) the Landau-Migdal spin-spin interaction strengths were fitted to experimental energies and $B(M1)$ values for 1^+ states in ^{48}Ca, ^{90}Zr, ^{208}Pb and to multipole splitting energies in ^{208}Bi and ^{40}K. The values, listed in Table I, are given with evaluated uncertainty: $g_0=0.04\pm0.08$, $g'=0.84\pm0.08$. This estimate for g_0 is in agreement with the microscopic values[26–29] and shows that small negative values[26,29] are also allowed. One should note, however, that the multipole

TABLE I. Review of different strength constants of the spin-spin interaction and numerical values for $A=130$. $c(+)=K_s/A$.

K_s (MeV)	$q=\frac{c(-)}{c(+)}$	g_0[a]	g'[a]	$c(+)$ (MeV) for $A=130$	$c(-)$ (MeV) for $A=130$	Ref.
236	$-0.25<q<0$			1.8	$-0.5\div0$	b
	$-0.50<q<0$			1.3	$-0.6\div0$	c
108[d]	0			0.8[d]	0	e
634	-0.33	0.49	0.98	4.9	-1.6	f
543	-0.11	0.56	0.70	4.2	-0.5	g
418	-0.12	0.42	0.54	3.2	-0.4	h
190	-1.54	-0.12	0.56	1.5	-2.2	i
237	-0.45	0.15	0.40	1.8	-0.8	j
203	-1.25	-0.06	0.53	1.6	-2.0	k
272	-0.59	0.13	0.49	2.1	-1.2	l
380	-0.91	0.04	0.84	2.9	-2.7	m

[a]The constants of the Landau-Migdal interaction are given in pionic normalization (Ref. 31): $C=392$ MeV fm^3. $K_s=1.1C(g_0+g')$ (MeV) with $r_0=1.2$ fm in Eq. (19).

[b]g factors of odd-mass nuclei with $150<A<190$ (Ref. 19).

[c]g factors and decoupling parameters of odd-mass nuclei with $150<A<190$ (Refs. 20–22); 1^+ states in even-even rare-earth nuclei (Refs. 2, 7, and 8), calculated with the constants of Refs. 20–22. $c(+)=(0.12-0.20)\hbar\omega$. We adopt here $0.16\hbar\omega$, $\hbar\omega=41A^{-1/3}$ MeV. Only the range $-0.25<q\leq0$ is allowed in Refs. 21 and 22.

[d]For $^{130}_{56}Ba_{74}$.

[e]$c(+)=6(N-Z)/A$ (Refs. 3 and 9).

[f]1^+ states in rare-earth nuclei (Ref. 12) with constants from description of magnetic moments of spherical and deformed nuclei.

[g]Electromagnetic transitions and g factors in ^{209}Bi, ^{207,208,209}Pb (Ref. 24).

[h]Collective excitations and electromagnetic transitions of nuclei from the Pb region (Ref. 25).

[i]Nuclear matter, G-matrix, Bonn potential, induced interactions, relativistic corrections (Ref. 29).

[j]Nuclear matter, G-matrix, Bonn potential, Brueckner-HF, relativistic corrections (Ref. 28).

[k]Pion condensation, nuclear matter, G-matrix, Bonn potential, BHF, first order induced interaction (Ref. 26).

[l]The same as k but the induced interaction is summed to all orders (Ref. 27).

[m]1^+ states in ^{48}Ca, ^{90}Zr, ^{208}Pb, multiplet splitting in ^{208}Bi, ^{40}K (Ref. 30).

splitting in ^{40}K allows g_0 values as large as 0.4.[30] The small g_0 values in the last five rows of Table I and especially cases k (Ref. 26) and m (Ref. 30) satisfy approximately the condition (13), since $|c(+)| \approx |c(-)|$ for $g_0 \approx 0$.

We calculated in QRPA the $M1$ strength distribution in ^{130}Ba with the formalism of Sec. II and different sets of spin-spin strengths. The results, obtained with the parameters of Sec. IV, are shown in Fig. 1. Case a corresponds to the Tübingen values[27] (l in Table I), case b to the Moscow values[30] (m in table I), case c to the Jülich results[19] (i in Table I), and d is the case without spin-spin interaction. It is seen from the figure, that the three different sets of constants of the spin-spin interaction (cases a, b, and c) produce very similar strength distributions, especially in the low-energy region 3–6 MeV. We adopted for our further calculations the Tübingen values[27] (case l in Table I) since their isovector-to-isoscalar q ratio (Table I) is in a better agreement with the phenomenological results from calculations of magnetic moments, decoupling parameters, and electromagnetic transitions (cases b, c, g, and h in Table I). Very similar values are obtained also in Ref. 28 (case j in Table I).

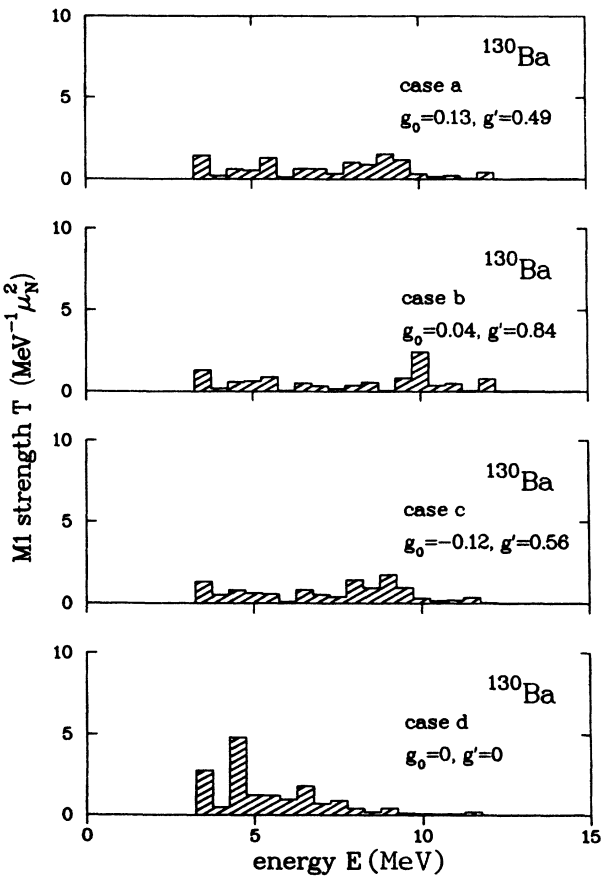

FIG. 1. Accumulated $M1$ strength distribution T [summed $B(M1)\uparrow$ values Eq. (16) of Ref. 11] per unit energy displayed in bins of 0.5 MeV for ^{130}Ba. The constants of the spin-spin interaction are from case a—Tübingen (Ref. 27) (l in Table I), case b—Moscow (Ref. 30) (m in Table I), case c—Jülich (Ref. 29) (i in Table I), case d—without spin-spin interaction.

IV. RESULTS AND DISCUSSION

The formalism, described in Sec. II, was used with a mean field generated from a deformed axially symmetric Woods-Saxon potential in cylindrical coordinates,[32] parametrized according to Ref. 33. Calculations have been performed for 16 even-even nuclei from the $A \approx 130$ mass zone: $^{120-132}$Xe, $^{126-134}$Ba, and $^{128-134}$Ce. Although the heavier Xe and Ba nuclei are not well deformed, the use of an axially symmetric mean field is still a reasonable approximation, because no definite evidence for a triaxial ground state is available, at least in the considered mass region.

A. The mean field parameters

The following parameters[33] of the Woods-Saxon potential were used for all the nuclei studied: $V_s = -50$ MeV, $V_d = -45$ MeV, $a_n = a_p = 0.63$ fm, $r_0^n = 1.27$ fm, $r_0^p = 1.24$ fm, $\lambda_0^n = 25$, $\lambda_0^p = 14$, $\hbar\omega_0 = 50A^{-1/3}$ MeV. These are the same parameters, as in our previous work,[15] except for a slight reduction of the oscillator constant $\hbar\omega_0$. It is known[33] that the results are not very sensitive to the oscillator strength. The above parameters are obtained by interpolation between the $A = 121$ and 141 mass zones of Ref. 34, except for the spin-orbit coupling constants $\lambda_0^{n,p}$, which are taken from Ref. 35. The small proton spin-orbit coupling constant is typical for microscopic calculations of 1^+ states in deformed nuclei.[11] Values, rounded to 0.1 MeV, were used for the BCS gap parameters of each nucleus, which were determined by reproducing roughly the even-odd mass differences.[36] The quadrupole deformation β_2, rounded to 0.01, was chosen for each nucleus to reproduce the experimental intrinsic quadrupole moment, derived from the $B(E2;0^+_{g.s.} \rightarrow 2^+_1)$ values.[37] The strengths of the quadrupole-quadrupole interaction H_{SCQ} (4) are not free parameters but are determined microscopically from an approximate condition of restoration of the rotational invariance.[11] The strengths of the rotation-vibrational coupling H_{RV} (4) are determined microscopically from the condition (5). Only the spin-spin interaction constants (1) are free parameters, taken from a previous work,[27] as explained in Sec. III.

B. Strongly orbital low-energy states

If only quadrupole-quadrupole H_{SCQ} and symmetry-restoring H_{RV} interactions are used without a spin interaction, the following typical features are observed in all the 16 nuclei studied (see, e.g., case d for ^{130}Ba on Fig. 2):

(i) The $M1$ strength is concentrated around 5 MeV, mostly in a single, well-pronounced peak. Only in $^{120-124}$Xe are there two additional comparable peaks: at 4 and 6 MeV.

(ii) The lowest-energy strong 1^+ states lie at 2.5–4 MeV. The first 2–3 of them (or at least 2–3 among the lowest 5–6 strong states) have a large orbit-to-spin ratio

R_{os} of the $M1$ matrix element, which means that they are predominantly orbital excitations.

(iii) At least one strong state with $B(M1)\uparrow \geq 1\mu_N^2$ is present between 4 and 5 MeV. In some nuclei there are two or three such states in this energy region. These are mainly excitations with a large spin contribution to the $M1$ matrix element ($|R_{os}|<1$), i.e., predominantly spin-flip transitions.

The above three main conclusions are in agreement with our previous results for $^{130-134}$Ba.[15] The strongly orbital character of the low-lying 1^+ states is a typical feature for the $A=130$ mass region and was not observed previously in the rare-earth[11,38] and $A=50$ (Refs. 18 and 38) mass regions. It is determined by the mean field and not by the residual interactions, because such states are present in calculations with different residual interactions: QQ, SS, QQ+SS, with or without the symmetry-restoring interaction H_{RV} (4). The low-energy strongly orbital states are built up from neutron quasiparticle pairs from the shells: $1h_{11/2}, 2d_{3/2}, 2d_{5/2}, 3s_{1/2}$ and pro-

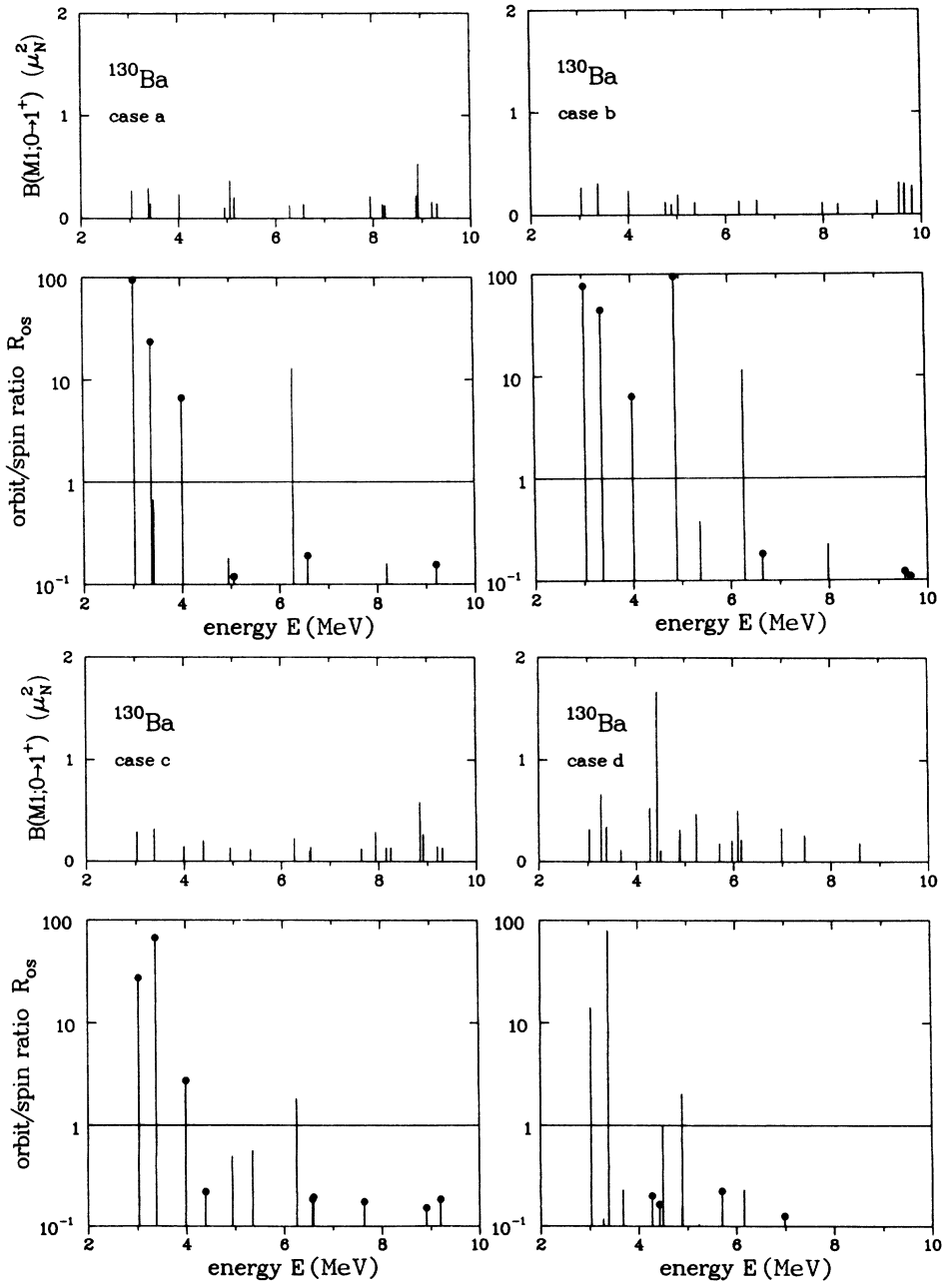

FIG. 2. Discrete $M1$ spectra for ^{130}Ba, corresponding to the four cases of Fig. 1, together with the respective orbit-to-spin ratios R_{os}, defined by Eq. (19) of Ref. 11. Only states with $B(M1)\uparrow > 0.1\mu_N^2$ are shown. Negative ratios R_{os} are indicated by a dot on the top of the bar and the absolute value is displayed.

ton quasiparticle pairs from $1g_{7/2}, 3d_{5/2}, 3s_{1/2}$. The strong orbital character is due to the fact that most of these pairs correspond to transitions between deformed orbitals, belonging to the same spherical shell.

C. Effects of the spin-spin interaction

The $M1$ strength distribution in ^{130}Ba, obtained with different spin-spin interaction constants and displayed in Fig. 1, was already discussed in the preceding section in connection with the choice of the interaction constants. One can see from Fig. 1 that the inclusion of the spin-spin interaction shifts the $M1$ strength up in energy, which has to be expected from a repulsive interaction. Moreover, the $M1$ strength is more uniformly distributed over a larger energy region: 3–10 MeV. The spin-spin interaction commutes with angular momentum operators. Thus, it can only redistribute the $M1$ strength but it does not create itself any $M1$ strength, because it does not contribute to the $M1$ energy-weighted sum rule. The $M1$ strength distribution for the Xe, Ba, and Ce nuclei studied is displayed in Figs. 3–5. The nuclei ^{128,130}Xe, which are very similar to ^{126}Xe, are not shown in order to save space. The results were obtained with the Tübingen spin-spin constants[27] given in case 1 of Table I.

More information can be obtained from Fig. 2, where the discrete low-energy (up to 8 MeV) $M1$ spectrum, corresponding to the four cases of Fig. 1, is shown. Only states with $B(M1)\uparrow > 0.1\mu_N^2$ are displayed. One can see

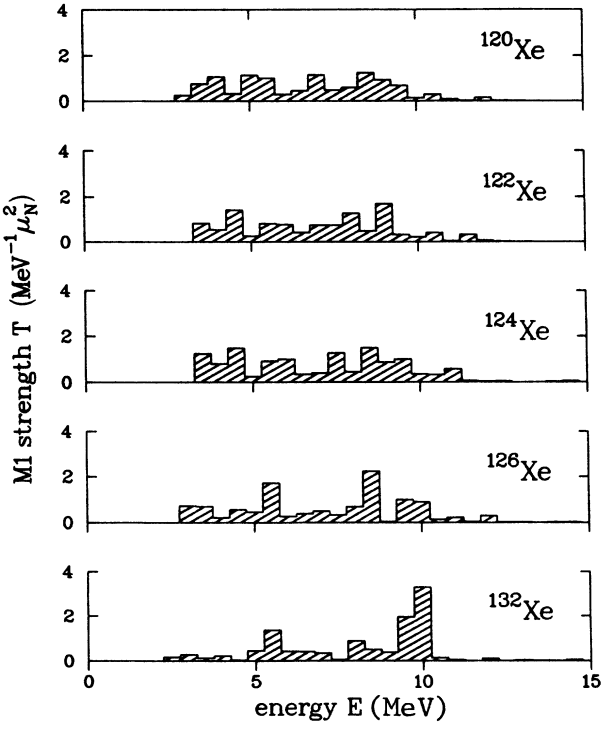

FIG. 3. $M1$ strength distribution for Xe nuclei, obtained with the spin-spin interaction constants from case 1 of Table I and displayed in bins of 0.5 MeV.

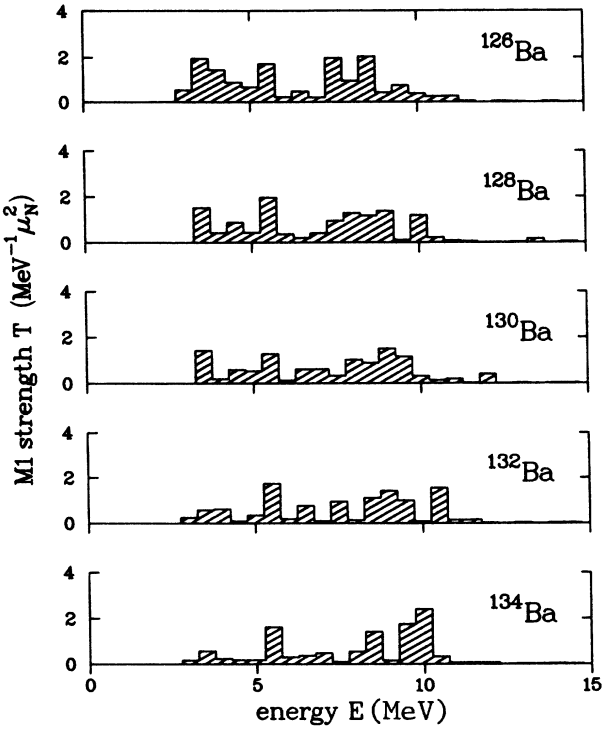

FIG. 4. The same as on Fig. 3 but for Ba nuclei.

that the spin-spin interaction suppresses the strong spin-flip transitions, which were present at 4–5 MeV with a QQ interaction only. The spin strength is now removed from the low-energy region to higher energies. As a result, the orbital character of the low-lying (2–5 MeV) 1^+ excitations is enhanced, while the higher-lying states acquire a more pronounced spin-flip nature. The spin-spin

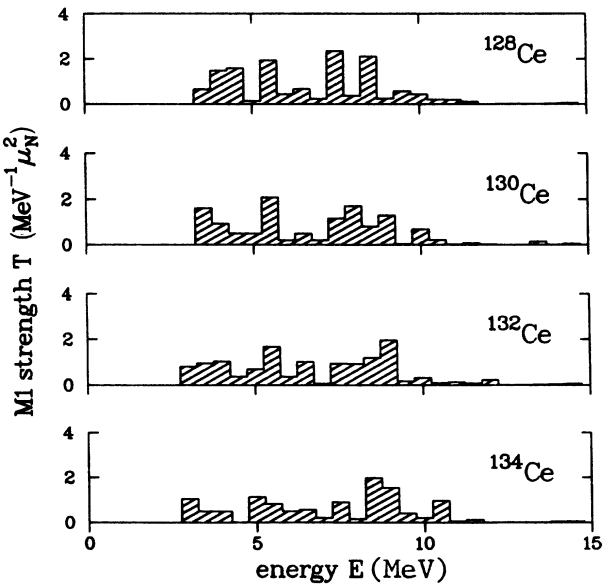

FIG. 5. The same as on Fig. 3 but for Ce nuclei.

interaction polarizes in this way the strong 1^+ excitations $[B(M1)\uparrow > 0.1\mu_N^2]$ in two distinct groups: low-lying states below 5 MeV, almost all of which are orbital in the 16 nuclei studied, and higher-lying states, almost all of which are spin-flip ($|R_{os}|<1$). Most of the orbital states have R_{os} of the order of 10, but states with $R_{os}=100$ are also present. The lowest-lying 1^+ states around 3 MeV are not very strong: The $B(M1)\uparrow$ value is typically $0.1-0.5\ \mu_N^2$.

One can see from Fig. 2 that different spin-spin coupling constants (cases a, b, and c) produce different $M1$ strength distribution in the higher energy (spin-flip) group of levels. On the other hand, the excitation energies, $B(M1)$ values, and orbit-to-spin ratios R_{os} of the low-energy orbital states are not much influenced by variation of the spin-spin coupling strengths. The first two states with a typical strongly orbital character are not much affected even if one switches off the spin-spin interaction. Its main effect on these states consists in the increase of their orbit-to-spin ratio due to a removal of spin strength from the $M1$ matrix element.

Predictions for the $M1$ strength distribution in $^{120-126}$Xe, $^{126-130}$Ba, and $^{128-134}$Ce were made previously[39] using the MONSTER approach. It consists of particle-number and spin-projected quasiparticle configurations, obtained from an HFB mean field and a Brueckner G matrix plus Bonn potential as a residual interaction. The $M1$ strength distribution, produced by this formalism, is centered around 4–5 MeV and is in a qualitative agreement with our results, obtained with a QQ interaction alone. This may be due to a weaker spin-spin term of the Bonn potential in comparison with our spin interaction strength. In both approaches the high-energy 1^+ states are mainly of spin-flip character. The main difference is in the orbit-to-spin ratio of the low-lying states. In the MONSTER approach these states have comparable orbital and spin contributions to the $M1$ matrix element or a dominant spin one, while in our approach the orbital contribution is always much stronger than the spin one. Possible reasons for this difference were already discussed elsewhere.[15] A microscopic realization of the Hamilton formalism in RPA and restoration of the invariance of the Hamiltonian with respect to the canonically conjugate angle can also hinder the spin-spin interaction under certain conditions. Further studies in this direction are under way.

V. COMPARISON WITH THE TWO-ROTOR MODEL

The two-rotor model[40] assumes an out-of-phase oscillation of the neutron and proton systems as a whole, which corresponds to a small-amplitude rotational vibration around an axis, perpendicular to the symmetry axis of the nucleus. Thus, in this geometrical model the whole strength of the 1^+ mode is concentrated in a single purely collective isovector state. Although in realistic microscopic calculations the rotational vibrations are fragmented over a broad region, the two-rotor model remains attractive due to its simple geometrical picture. In order to interpret geometrically our microscopic results we need a microscopic realization of the purely collective isovector state of the macroscopic two-rotor model. There is no spin degree of freedom in this model. Therefore, the rotations are generated by the orbital angular momentum operator L. However, in a microscopic formalism, where spin degrees of freedom are present as well, one has to use the total angular momentum $I=L+S$. The purely collective isovector rotational (ROT) and orbital (ORB) states are constructed microscopically from the I and L operators, respectively, as normalized isovector wave functions, which are orthogonal to the spurious isoscalar rotational state (IS), generated by I:[40]

$$
\begin{aligned}
&|\mathrm{IS},m\rangle=\frac{1}{\sqrt{P_j}}[I^\dagger(m,n)+I^\dagger(m,p)]|\rangle\ ,\\
&|\mathrm{ROT},m\rangle=\frac{1}{\sqrt{P_j}}[\sqrt{P_j(p)/P_j(n)}I^\dagger(m,n)-\sqrt{P_j(n)/P_j(p)}I^\dagger(m,p)]|\rangle\ ,\\
&P_j=P_j(n)+P_j(p),\quad \langle \mathrm{IS},m|\mathrm{ROT},m'\rangle=0 \ \text{ for any } m,m'=\pm1\ ,\\
&|\mathrm{ORB},m\rangle=N[b(n)L^\dagger(m,n)-b(p)L^\dagger(m,p)]|\rangle\ ,\\
&\langle \mathrm{IS},m|\mathrm{ORB},m'\rangle=0 \ \text{ for any } m,m'=\pm1\ ,\\
&N=P_L^{-1/2},\quad b(n)=P_{lj}(p),\quad b(p)=P_{lj}(n)\ ,\\
&P_L=P_{lj}^2(p)P_l(n)+P_{lj}^2(n)P_l(p)\ ,\\
&P_{lj}(t)=2\sum_{ik}[l(ki,mt)j(ki,mt)+l(\tilde{ki},mt)j(\tilde{ki},mt)],\quad t=n,p\ .
\end{aligned}
\tag{21}
$$

The sums P_l and P_j are obtained from P_{lj} (21) by the substitutions $j\to l$ and $l\to j$, respectively. The angular momentum operators (21) are taken in quasiboson approximation,[11] which is usual for the RPA approach. The microscopic purely collective isovector states ROT and ORB (21) correspond in our case to rotation of the deformed Woods-Saxon ground state density distribution around an axis perpendicular to the symmetry axis of the nucleus. In contrast to the 1^+ state of the two-rotor model, which is purely orbital and has no spin contribu-

TABLE II. Comparison between the RPA and the purely collective rotational ROT and orbital ORB (21) isovector vibrations in ^{130}Ba. The states RPA_1 and RPA_2 are obtained with QQ+SS+RV (4) residual interactions, RPA_3 is obtained without SS interaction and corresponds to RPA_2. ROT and ORB are generated directly from the mean field H_0 without using the RPA procedure of solving the secular equation.

State	E (MeV)	$B(M1)\uparrow$ (μ_N^2)	R_{os}	$\lvert\langle$state$\rvert$ROT$\rangle\rvert^2$ (%)
RPA_1	3.03	0.27	−105.3	12
RPA_2	8.92	0.52	−0.1	0
RPA_3	4.43	1.67	−0.2	1
ROT	6.80	2.35	18.7	100
ORB	6.86	0.49	−1.9	91

tion, the microscopic state ORB contains a large amount of spin (see, e.g., the comparable orbital and spin contributions to the $M1$ matrix element of the ORB state in Table II). On the other hand, the strongly orbital ROT state can be considered as being the microscopic realization of the scissor 1^+ state from the two-rotor model. These two states are obtained from the mean field H_0 (4) and not from the RPA equations of motion (7). They are compared in Table II to typical RPA states, obtained with QQ+SS+RV interactions (the first two rows): RPA_1 is the lowest-lying (at about 3 MeV) strong $M1$ state, which is also strongly orbital, while the strongest $M1$ state RPA_2 lies at 8.9 MeV and it is of spin-flip nature. These two RPA states have in ^{130}Ba the following leading $2qp$ components of their wave functions:

$E_1 = 3.0$ MeV

$$-34\%nn[523]_{\frac{7}{2}},[514]_{\frac{9}{2}},\quad +25\%pp[420]_{\frac{1}{2}},[411]_{\frac{3}{2}},$$

$$-14\%nn[532]_{\frac{5}{2}},[523]_{\frac{7}{2}},\quad +15\%pp[422]_{\frac{3}{2}},[413]_{\frac{5}{2}},$$

$E_2 = 8.9$ MeV

$$-35\%nn[503]_{\frac{7}{2}},[514]_{\frac{9}{2}},$$

$$+28\%pp[440]_{-\frac{1}{2}},[431]_{\frac{1}{2}}.$$

We calculated the transverse $M1$ transition densities and form factors for inelastic electron scattering, corresponding to the strong RPA rotational vibrations, as well as to the purely collective isovector states ROT and ORB (21). The densities were obtained using the formalism of Ref. 18 and the cross sections—with the DWBA code of Heisenberg.[41] The transition densities and form factors of the collective states ROT and ORB are very similar, as one can see from Figs. 6 and 7. These two states overlap 91% with each other (Table II).

The RPA results show (e.g., Figs. 6 and 7) that the (e,e') form factors of the strongly orbital low-lying 1^+ RPA states are very similar to the form factors of the purely collective states ROT and ORB, although smaller in magnitude. The results for ^{130}Ba, displayed in Figs. 6 and 7, are obtained with QQ+SS+RV interactions (case a on Fig. 1) with coupling constants from case 1 in Table I. The DWBA (e,e') transverse $M1$ transition densities are displayed in Fig. 6 and the corresponding form factors in Fig. 7. The form factor of the low-energy state RPA_1 at 3 MeV is shown on the left-hand side (lhs), while the form factor on the rhs corresponds to the strongest 1^+ state RPA_2 at 8.9 MeV. Both RPA form factors (continuous lines) are compared in Fig. 7 to those of the purely collective microscopic isovector states ROT (dot-dashed line) and ORB (dashed line). One can see from Figs. 6 and 7 that the strongly orbital RPA state at 3 MeV is similar to the purely collective states ROT and ORB, while the strong spin RPA_2 state at 8.9 MeV is very different from the purely collective states. Without a spin-spin interaction the strongest $M1$ state moves from 8.9 to about 4.4 MeV (this is the state RPA_3 in Table II), has a larger $B(M1)$ value, and a larger overlap with the ROT state.

The smaller form factor of the RPA_1 state in comparison with the collective form factor is due to the lower degree of collectivity of the RPA excitation, which leads also to a very small overlap (12%, Table II) with the ROT wave function. Nevertheless, the similarity between

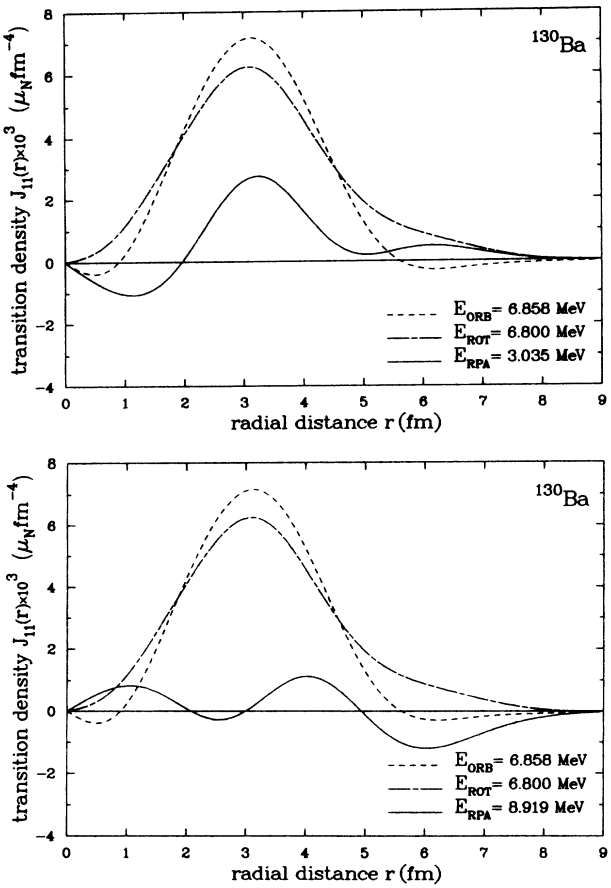

FIG. 6. Transverse $M1$ transition density for the purely collective isovector rotational ROT and orbital ORB states (21), as well as for the RPA rotation-vibrational 1^+ states RPA_1 at 3 MeV (upper) and RPA_2 at 7.2 MeV (lower). Results for ^{130}Ba, obtained with the spin-spin interaction constants from case 1 of Table I.

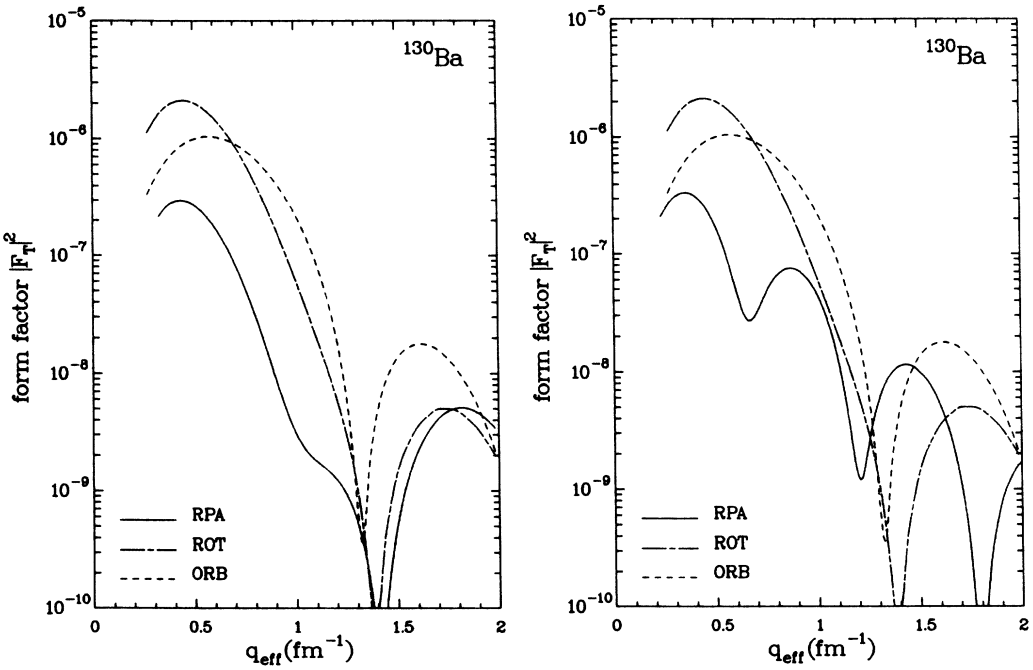

FIG. 7. Transverse $M1$ form factor for inelastic electron scattering, calculated in DWBA with the transition densities, corresponding to the ROT, ORB, and the RPA states from Fig. 6 (RPA_1 is on the lhs, RPA_2 on the rhs).

the transition density of the purely collective state and the orbital RPA_1 state shows that the low-energy RPA excitation performs scissor-type rotational vibrations, corresponding to the geometrical motion of the two-rotor model. The form factor of the second low-energy RPA state at 3.4 MeV, which is not displayed on Fig. 7, is even more similar to the collective form factor than that of the first RPA state. Both RPA states are strongly orbital, as one can see from Fig. 2, case a.

Thus, the low-energy RPA states in the studied $A=130$ mass region are strongly orbital and have (e,e') form factors, which are smaller in magnitude but similar to the form factor of the purely collective scissor state. This means that the low-energy RPA excitations perform rotational vibrations—the geometrical type of motion, inherent to the two-rotor model, but only few quasiparticles are participating in this motion, while all the particles contribute to the purely collective scissor state.

VI. CONCLUSIONS

A quasiparticle RPA approach is used to study the isovector rotational vibrations ($K^\pi=1^+$ states) in 16 even-even nuclei from the $A=130$ mass region: $^{120-132}$Xe, $^{126-134}$Ba, and $^{128-134}$Ce. The mean field is described by an axially symmetric deformed Woods-Saxon potential in cylindrical coordinates. The residual interaction includes a quadrupole-quadrupole force, a spin-spin force, and a rotation-vibrational coupling, which restores the rotational invariance of the Hamiltonian, broken by the mean field and the QQ force. The strength constants of the SS interaction are taken from other microscopic calculations,[27] while the coupling constants of the remaining residual interactions are determined microscopically in our formalism from the condition of rotational symmetry restoration.

In contrast to the rare-earth[11] and the $A=50$ (Ref. 18) mass regions, a well-pronounced shell effect is found, which is typical for the $A=130$ mass region: Regardless of the residual interactions used, strongly orbital rotational vibrations are present at low excitation energy (below 5 MeV). This means that the orbital contribution to the $M1$ transition matrix element is much larger than the spin contribution. The effect is due to the fact that in this mass region the low-energy $|\Delta\Omega|=1$ transitions take place between deformed orbitals, belonging to the same spherical shell, and admixtures from adjacent shells are not strong.

The inclusion of the spin-spin force moves the spin strength from lower to higher energies. As a result:

(i) The orbital character of the low-lying (2–5 MeV) 1^+ excitations is enhanced, while the higher-lying ones acquire a more pronounced spin-flip nature. Almost all of the 1^+ states below 5 MeV become strongly orbital, while almost all of the higher-lying states become predominantly spin-flip.

(ii) The strongly orbital states, having a small spin contribution, are not much affected by the SS interaction, which influences stronger states with large spin contribution (spin-flip states).

Without a spin-spin force the $M1$ strength distribution is concentrated around 5 MeV, usually in a single, well-pronounced peak. The SS interaction does not contribute to the $M1$ energy-weighted sum rule. Therefore, it only redistributes but does not create an $M1$ strength. When included, this repulsive interaction shifts the $M1$ strength up in energy and redistributes it more uniformly over the 3–10 MeV energy region. The results, obtained with a

spin-spin force, must be taken with some cautiousness because its coupling constants are free parameters.

A microscopic realization of the purely collective isovector rotational state of the two-rotor model[40] is proposed, which corresponds to a contrarotation of the neutron and proton components of the deformed mean field. In contrast to the macroscopic two-rotor model, where no spin degrees are present and the collective 1^+ state is purely orbital by definition, the microscopic realization of this geometrical motion leads to a wave function with a small spin contribution to the $M1$ transition matrix element and predominantly orbital character. A formalism is developed, which allows us to treat microscopically the purely collective 1^+ state on an equal footing with the RPA 1^+ excitations. The $M1$ transition densities and (e,e') form factors, calculated in DWBA, show that the strongly orbital low-energy RPA excitations cannot be identified with the purely collective isovector rotational state, lying at about 7 MeV, since only few nucleons take part in a given RPA excitation. Each one of these RPA states overlaps only about 10–15 % with the purely collective isovector vibration. However, the low-energy RPA states have form factors, which are similar to the form factors of the purely collective scissor state, although smaller in magnitude. The small overlap with the purely collective state and the smaller $B(M1)$ value show that the RPA state has a lower degree of collectivity, which can be seen also by comparing the two wave functions. Nevertheless, the similarity of the form factors and transition densities indicates that the low-energy orbital RPA excitations perform a scissor-type or rotational vibration—the geometrical type of motion, predicted by the two-rotor model. The form factors of the higher-energy RPA states, which are spin-flip excitations, do not exhibit such a similarity with the form factor of the purely collective scissor state.

The above identification does not exclude the possibility that other RPA states perform the same kind of geometrical motion. Only a few quasiparticle pairs take part in a given RPA 1^+ excitation. Thus, a contrarotation of only a few orbitals may produce a current, which can be very different from the current, corresponding to the contrarotation of the whole ground state density, described by the purely collective isovector rotational state.

ACKNOWLEDGMENTS

Thanks are due to A. Arima, S. Gabrakov, N. Pyatov, and K. Schmid for useful discussions. One of us (R.N.) acknowledges a research grant from the Alexander von Humboldt Foundation. This work was supported by the Alexander von Humboldt Foundation and the Federal Ministry of Research and Technology (Federal Republic of Germany) under Contract No. 06 Tü 778.

APPENDIX

The determinant of the RPA linear homogeneous system of Eqs. (5 and 6) with respect to the unknowns $N(\nu,n)$, $N(\nu,P)$, $L(\nu,m,n)$, $L(\nu,m,p)$, and $k(\nu,m)$ has the form

$$\begin{vmatrix} 1-k(+,n)A^n_{qq} & -k(-)A^p_{qq} & k(+,n)W_\nu A^n_{qs} & k(-)W_\nu A^p_{qs} & W_\nu T^n_q \\ -k(-)A^n_{qq} & 1-k(+,p)A^p_{qq} & k(-)W_\nu A^n_{qs} & k(+,p)W_\nu A^p_{qs} & W_\nu T^p_q \\ -c(+,n)W_\nu A^n_{qs} & -c(-)W_\nu A^p_{qs} & 1+c(+,n)A^n_{ss} & c(-)A^p_{ss} & T^n_s \\ -c(-)W_\nu A^n_{qs} & -c(+,p)W_\nu A^p_{qs} & c(-)A^n_{ss} & 1+c(+,p)A^p_{ss} & T^p_s \\ -W_\nu A^n_{qj} & -W_\nu A^p_{qj} & A^n_{sj} & A^p_{sj} & A^n_{jj}+A^p_{jj} \end{vmatrix} , \tag{A1}$$

$$T^t_q = k(+,t)A^t_{qj} + k(-)A^{-t}_{qj}, \quad T^t_s = c(+,t)A^t_{sj} + c(-)A^{-t}_{sj} ,$$

where the phonon-dependent microscopic sums A^t_{uv} ($t=n,p$; the ν index omitted) are defined in the following way:

$$A^t_{uv} = 4\sum_{ik} E(ik)[u(ki,mt)v(ki,mt)+u(\tilde{k}i,mt)v(\tilde{k}i,mt)]/[E^2(ik)-W^2_\nu], \quad \text{for } (uv)=(qq),(jj),(ss),(sj) ,$$
$$A^t_{uv} = 4\sum_{ik} [u(ki,mt)v(ki,mt)+u(\tilde{k}i,mt)v(\tilde{k}i,mt)]/[E^2(ik)-W^2_\nu], \quad \text{for } (uv)=(qs),(qj) . \tag{A2}$$

The analytical form (10) of the secular equation, resulting from the above determinant equal to zero, requires to define the following sums, used in (10):

$$B_{qq}(\pm,t) = k(\pm,t)A^t_{qq} - W^2_\nu A^t_{qj} T_q(\pm,t)/A_{jj} ,$$
$$B_{qj}(\pm,t) = k(\pm,t)A^t_{sq} - A^t_{sj} T_q(\pm,t)/A_{jj} ,$$
$$B_{ss}(\pm,t) = c(\pm,t)A^t_{ss} - A^t_{sj} T_s(\pm,t)/A_{jj} ,$$
$$B_{sj}(\pm,t) = c(\pm,t)A^t_{sq} - A^t_{qj} T_s(\pm,t)/A_{jj} , \tag{A3}$$
$$T_q(\pm,t) = k(\pm,t)A^t_{qj} + k(\mp,-t)A^{-t}_{qj}, \quad T_s(\pm,t) = c(\pm,t)A^t_{sj} + c(\mp,-t)A^{-t}_{sj} ,$$
$$A_{jj} = A^n_{jj} + A^p_{jj}, \quad k(-,t) = k(-,-t) \equiv k(-), \quad -t = \begin{cases} n, & \text{for } t=p , \\ p, & \text{for } t=n . \end{cases}$$

One can easily check that:

$$T(-,t)=T(+,-t)\ . \tag{A4}$$

In the particular case of self-consistently chosen interaction constants (11) for the QQ interaction and/or $c(+,n)c(+,p)=c^2(-)$ for the SS interaction, the following symmetries arise:

$$\begin{aligned}
&B_{qv}(-,t)=B_{qv}(+,t)k(-)/k(+,t)\ ,\\
&B_{sv}(-,t)=B_{sv}(+,t)c(-)/c(+,t),\quad v=q,j\ ,\\
&p(q,t)=B_{qj}(+,t),\quad v(q,t)=B_{qj}(-,t)=p(q,t)k(-)/k(+,t)\ ,
\end{aligned} \tag{A5}$$

$$D=0\ , \tag{A6}$$

and analogous relations for $p(s,t)$ and $v(s,t)$.

The following relations between $N(\nu,n)$, $N(\nu,p)$, $L(\nu,m,n)$, $L(\nu,m,p)$, and $k(\nu,m)$ can be derived from the linear system, whose determinant is given by (A1):

$$\begin{aligned}
&N(\nu,p)=a(\nu)N(\nu,n),\quad k(\nu,m)=\bar{k}(\nu,m)N(\nu,n)\ ,\\
&L(\nu,m,n)=l(n)N(\nu,n),\quad L(\nu,m,p)=l(p)N(\nu,n)\ ,\\
&a(\nu)=\{gB_{qq}(-,n)-W_\nu^2F(p)\}/\{g[1-B_{qq}(+,p)]+W_\nu^2G(p)\}\\
&\quad=\{g[1-B_{qq}(+,n)]+W_\nu^2G(n)\}/\{gB_{qq}(-,p)-W_\nu^2F(n)\}\ ,\\
&F(t)=v(s,-t)B_{qj}(+,t)+p(s,-t)B_{qj}(-,-t)\ ,\\
&G(t)=p(s,t)B_{qj}(+,t)+v(s,t)B_{qj}(-,-t)\ ,\\
&l(n)=[p(s,n)+a(\nu)v(s,p)]W_\nu/g,\quad l(p)=[p(s,p)a(\nu)+v(s,n)]W_\nu/g\ ,\\
&\bar{k}(\nu,m)=\{W_\nu[A_{qj}^n+a(\nu)A_{qj}^p]-l(n)A_{sj}^n-l(p)A_{sj}^p\}/A_{jj}
\end{aligned} \tag{A7}$$

These relations allow us to determine all the norms and $k(\nu,m)$ from the normalization condition (7), which has the form

$$\begin{aligned}
&\tfrac{1}{2}\sum_t\{W_\nu N^2(\nu,t)A_{qq}^{\prime t}+W_\nu L^2(\nu,m,t)A_{ss}^{\prime t}+W_\nu k^2(\nu,m)A_{jj}^{\prime t}\\
&\qquad+2k(\nu,m)L(\nu,m,t)W_\nu A_{sj}^{\prime t}-N(\nu,t)L(\nu,m,t)A_{qs}^{\prime t}-k(\nu,m)N(\nu,t)A_{qj}^{\prime t}\}=1\ ,\\
&A_{uv}^{\prime t}=\frac{1}{2W}\frac{\partial}{\partial W}A_{uv}^t,\quad \text{for } (uv)=(qq),(jj),(ss),(sj)\ ,\\
&A_u^{\prime t}=\frac{\partial}{\partial W}(WA_{uv}^t),\quad \text{for } (uv)=(qs),(qj)\ ,
\end{aligned} \tag{A8}$$

where the sums A_{uv}^t are defined by (A2). Using the relations (A7) one can eliminate all the unknowns from (A8) but $N(\nu,m)$, which will be determined therefore from this equation. Once $N(\nu,n)$ is obtained from (A8), the remaining four unknowns $N(\nu,p)$, $L(\nu,m,n)$, $L(\nu,m,p)$, and $k(\nu,m)$ are found from (A7).

---

*Permanent address: Institute of Nuclear Research and Nuclear Energy, Bulgarian Academy of Sciences, Sofia 1784, Bulgaria.

[1]A. Bohr and B. Mottelson, *Nuclear Structure* (Benjamin, New York, 1974) Vol. 2.
[2]S. I. Gabrakov, A. A. Kuliev, and N. I. Pyatov, Yad. Fiz. **12**, 82 (1970).
[3]S. I. Gabrakov, A. K. Kuliev, N. I. Pyatov, D. I. Salamov, and H. Schulz, Nucl. Phys. **A182**, 625 (1972).
[4]R. A. Broglia, A. Molinari, and B. Sørensen, Nucl. Phys. **A109**, 353 (1968).
[5]A. Faessler, Nucl. Phys. **85**, 653 (1966); A. Faessler and R. Nojarov, Phys. Lett. **166B**, 367 (1986); R. Nojarov and A. Faessler, J. Phys. G **13**, 337 (1987).
[6]V. M. Mihailov, Izv. Akad. Nauk. SSSR, Ser. Fiz. **34**, 840 (1970).
[7]V. M. Mihailov and V. V. Pogossyan, Yad. Fiz. **16**, 289 (1972).
[8]N. I. Pyatov and M. I. Chernej, Yad. Fiz. **16**, 931 (1972).
[9]A. A. Kuliev and N. I. Pyatov, Yad. Fiz. **20**, 297 (1974).
[10]S. Iwasaki and K. Hara, Phys. Lett. **144B**, 9 (1984).
[11]R. Nojarov and A. Faessler, Nucl. Phys. **A484**, 1 (1988).
[12]B. L. Birbrair and K. N. Nikolaev, Yad. Fiz. **14**, 705 (1971).
[13]D. Zawischa, J. Speth, and D. Pal, Nucl. Phys. **A311**, 445 (1978).
[14]E. R. Marshalek and J. Weneser, Ann. Phys. (N.Y.) **53**, 569 (1969).
[15]H. Harter, P. O. Lipas, R. Nojarov, T. Taigel, and A. Faessler, Phys. Lett. B **205**, 174 (1988).

[16]C. Djalali, N. Marty, M. Morlet, A. Willis, J. C. Jourdain, D. Bohle, U. Hartmann, G. Küchler, A. Richter, G. Caskey, G. M. Grawley, and A. Galonsky, Phys. Lett. **164B**, 269 (1985).
[17]C. Wesselborg, K. Schiffer, K. O. Zell, P. von Brentano, D. Bohle, A. Richter, G. P. A. Berg, B. Brinkmöller, J. G. M. Römer, F. Osterfeld, and M. Yabe, Z. Phys. A **323**, 485 (1986).
[18]A. Faessler, R. Nojarov, and T. Taigel, Nucl. Phys. **A492**, 105 (1989).
[19]Z. Bochnacki and S. Ogaza, Nucl. Phys. **69**, 186 (1965).
[20]A. A. Kuliev and N. I. Pyatov, Yad. Fiz. **9**, 313 (1968).
[21]A. A. Kuliev and N. I. Pyatov, Yad. Fiz. **9**, 955 (1968).
[22]A. A. Kuliev and N. I. Pyatov, Phys. Lett. **28B**, 443 (1969).
[23]P. Ring and J. Speth, Phys. Lett. **44B**, 477 (1973).
[24]J. Speth, E. Werner, and W. Wild, Phys. Rep. **33**, 127 (1977).
[25]G. A. Rinker and J. Speth, Nucl. Phys. **A306**, 360 (1978).
[26]W. H. Dickhoff, A. Faessler, J. Meyer-Ter-Vehn, and H. Müther, Nucl. Phys. **A368**, 445 (1981).
[27]W. H. Dickhoff, A. Faessler, H. Müther, and S. S. Wu, Nucl. Phys. **A405**, 534 (1983).
[28]M. R. Anastasio, L. S. Celenza, W. S. Pong, and C. M. Shakin, Phys. Rep. **100**, 327 (1983).
[29]K. Nakayama, S. Krewald, and J. Speth, Phys. Lett. **145B**, 310 (1984).
[30]I. N. Borzov, S. V. Tolokonnikov, and S. A. Fayans, Yad. Fiz. **40**, 1151 (1984).
[31]I. S. Towner, Phys. Rep. **155**, 263 (1987).
[32]J. Damgaard, H.-C. Pauli, V. V. Pashkevich, and V. M. Strutinski, Nucl. Phys. **A135**, 432 (1969).
[33]R. Nojarov, J. Phys. G **10**, 539 (1984).
[34]V. Yu. Ponomarev, V. G. Soloviev, Ch. Stoyanov, and A. I. Vdovin, Nucl. Phys. **A323**, 446 (1979).
[35]J. Dudek and T. Werner, J. Phys. G **4**, 1543 (1978).
[36]A. H. Wapstra and G. Audi, Nucl. Phys. **A432**, 1 (1985).
[37]S. Raman, C. H. Malarkey, W. T. Milner, C. W. Nestor, Jr., and P. H. Stelson, At. Data Nucl. Data Tables **36**, 1 (1987).
[38]A. Faessler and R. Nojarov, Prog. Part. Nucl. Phys. **19**, 167 (1987); R. Nojarov, A. Faessler, and O. Civitarese, Phys. Lett. B **183**, 122 (1987).
[39]E. Hammaren, K. W. Schmid, A. Faessler, and F. Grümmer, Phys. Lett. B **171**, 347 (1986).
[40]N. Lo Iudice and F. Palumbo, Phys. Rev. Lett. **41**, 1532 (1978); Nucl. Phys. **A326**, 193 (1979); G. de Franceschi, N. Lo Iudice, and F. Palumbo, Phys. Rev. C **29**, 1496 (1984).
[41]J. Heisenberg and H. P. Blok, Annu. Rev. Nucl. Part. Sci. **33**, 569 (1983).